ELSEVIER

Mutation Research 460 (2000) 277–300

DNA Repair

www.elsevier.com/locate/dnarepair
Community address: www.elsevier.com/locate/mutres

The nucleotide excision repair protein UvrB, a helicase-like enzyme with a catch

Karsten Theis [a], Milan Skorvaga [b,c], Mischa Machius [d], Noriko Nakagawa [e], Bennett Van Houten [b], Caroline Kisker [a,*]

[a] *Department of Pharmacological Sciences, State University of New York at Stony Brook, Stony Brook, NY 11794-8651, USA*
[b] *Laboratory of Molecular Genetics, National Institute of Environmental Health Sciences, National Institutes of Health, Research Triangle Park, NC 27709, USA*
[c] *Department of Molecular Genetics, Cancer Research Institute, Slovak Academy of Sciences, Vlarska 7, 833 91 Bratislava, Slovak Republic*
[d] *Howard Hughes Medical Institute and Department of Biochemistry, University of Texas Southwestern Medical Center at Dallas, 5323 Harry Hines Boulevard, Dallas, TX 75235-9050, USA*
[e] *Department of Biology, Graduate School of Science, Osaka University, Toyonaka, Osaka, 560-0043, Japan*

Abstract

Nucleotide excision repair (NER) is a universal DNA repair mechanism found in all three kingdoms of life. Its ability to repair a broad range of DNA lesions sets NER apart from other repair mechanisms. NER systems recognize the damaged DNA strand and cleave it 3′, then 5′ to the lesion. After the oligonucleotide containing the lesion is removed, repair synthesis fills the resulting gap. UvrB is the central component of bacterial NER. It is directly involved in distinguishing damaged from undamaged DNA and guides the DNA from recognition to repair synthesis. Recently solved structures of UvrB from different organisms represent the first high-resolution view into bacterial NER. The structures provide detailed insight into the domain architecture of UvrB and, through comparison, suggest possible domain movements. The structure of UvrB consists of five domains. Domains 1a and 3 bind ATP at the inter-domain interface and share high structural similarity to helicases of superfamilies I and II. Not related to helicase structures, domains 2 and 4 are involved in interactions with either UvrA or UvrC, whereas domain 1b was implicated for DNA binding. The structures indicate that ATP binding and hydrolysis is associated with domain motions. UvrB's ATPase activity, however, is not coupled to the separation of long DNA duplexes as in helicases, but rather leads to the formation of the preincision complex with the damaged DNA substrate. The location of conserved residues and structural comparisons with helicase–DNA structures suggest how UvrB might bind to DNA. A model of the UvrB–DNA interaction in which a β-hairpin of UvrB inserts between the DNA double strand has been proposed recently. This padlock model is developed further to suggest two distinct consequences of domain motion: in the $UvrA_2B$–DNA complex, domain motions lead to translocation along the DNA, whereas in the tight UvrB–DNA pre-incision complex, they lead to distortion of the 3′ incision site.

Keywords: DNA damage; Nucleotide excision repair; Helicase; Domain motion; ATPase; UvrB

* Corresponding author. Tel.: +1-631-632-14-65; fax: +1-631-444-3218.
E-mail address: kisker@pharm.sunysb.edu (C. Kisker).

0921-8777/00/$ - see front matter
PII: S0921-8777(00)00032-X

1. Introduction

Among the various DNA repair mechanisms available to the cell, nucleotide excision repair (NER) stands out because of its broad substrate specificity (Table 1). NER removes damaged DNA through excision of an oligonucleotide that contains the lesion. Although the proteins involved are different, eukaryotic and prokaryotic cells share this basic mechanism. NER in bacteria, one of the first repair mechanisms discovered [1,2], is mediated by the gene products of the *uvrA*, *uvrB*, and *uvrC* genes [3–5]. The proteins UvrA, UvrB and UvrC recognize and cleave the damaged DNA in a multi-step, ATP-dependent reaction (Fig. 1a). In vitro studies with purified proteins showed that the reconstituted UvrABC proteins cleave both sides of the damaged strand several nucleotides away from the lesion [6]. Potential problems in processing these modifications, e.g. inhibition of the endonuclease activities by certain lesions are elegantly circumvented by cleaving at a distance from the lesion [6]. Thus, the NER mechanism is ideally suited to process a wide variety of modifications once they have been recognized.

The recognition of damaged DNA is a multi-step process in itself (Fig. 1a). At physiological concentrations, UvrA is bound to UvrB in the ternary $UvrA_2B$ complex; this presumably is the complex that initially binds to DNA [7]. UvrA is able to bind preferentially to damaged DNA even in the absence of UvrB, but high specificity of damage recognition requires the interplay of UvrA and UvrB. The footprint of UvrA bound to site-specifically damaged DNA changes from 33 to 19 bp when UvrB is added [8]. This equivocal footprint was found to be due to dissociation of UvrA from the nucleoprotein complex leading to formation of a stable UvrB·DNA pre-incision complex [7,9].

After UvrC binds to the pre-incision complex, it first cuts on the 3′ side and then on the 5′ side of the

Table 1
Range of substrates of the bacterial NER UvrABC system

Type	Lesion	UvrABC	ΔM_r	Properties
Single base modification	Thymine glycol	+ +	+34	
	Dihydrothymine	0	+2	
	Benzo[*a*]pyrene adduct	+ + +	+171	T_M lowered
	Anthramycin adduct	+ + +	+191	T_M elevated
	cross linked triple strand	+ [72]	~ +3000	
	O^4-alkyl thymine	+	+14	
	O^6-methyl guanine	+	+14	
	N^6-methyl adenine	0	+14	
	Psoralen adduct	+ + +	+185	Positive kink
	Base removed (AP site)	+	~ −130	
Cross-links, intra-strand	*cis*-Pt adduct	+ + +	+227	Negative kink
	Pyrimidine dimer	+ +	0	
	6–4 photoproduct	+ + +	0	
Cross-links, inter-strand	*cis*-Pt adduct	+ +	+227	
	Nitrogen mustard adduct	+	+69	
	Psoralen bisadduct	+ + +	+185	unwound
Natural bases[a]	dsDNA	0	0	
	A-tracts	0	0	bent
	Mismatches, loops	0[b]	0	
Non-covalent modifications	Caffeine complex	−	+194	intercalator
	Ditercalinium complex	+ +[c]	+500	bisintercalator

A selection of DNA lesions (for an extensive list and references, see Refs. [17,71]) illustrates the lack of a single common property that determines the response of UvrABC to DNA damage. The relative rate of incision for a particular lesion (neglecting the influence of sequence context) by the UvrABC system is indicated by +, + +, and + + +; 0 indicates no incision, · indicates inhibition. ΔM_r, change in molecular weight due to the modification.

[a] See Table 3.

[b] Some mismatches are recognized with very low efficiency (< 1%).

[c] Futile cycle of spurious repair and subsequent formation of the complex at another site.

lesion. Sequence comparisons and site-directed mutagenesis showed that both the 3′ and the 5′ incision are catalyzed by UvrC, which contains two separate catalytic sites that can be inactivated independently of each other [10,11]. Soon after the incision activity of the UvrABC system was discovered, it became clear that UvrD and DNA polymerase I are required for turnover of the Uvr proteins [12,13]. Subsequent studies indicated that the helicase UvrD removes both UvrC and the oligonucleotide containing the lesion, while UvrB remains bound to the gapped DNA until the gap is filled by DNA polymerase I [14]. Finally, DNA ligase closes the nicked DNA. Thus, there is a division of labor between the UvrABC proteins, with UvrA and UvrB recognizing and UvrC hydrolyzing the damaged DNA. As the central component of the repair cascade, UvrB interacts with UvrA, UvrC and DNA. In addition to its role in recognition of damage, UvrB guides the DNA from recognition to repair synthesis, ensuring that no gapped DNA intermediates are released before the repair pathway is completed.

Preferential repair of the coding strand of transcribed genes led to the discovery of a second recognition pathway, which is initiated by RNA polymerase stalled at a lesion (Fig. 1a). The Mfd protein binds to this site, removes RNA polymerase from the lesion and presumably recruits UvrA and UvrB [15]. Although only a few intermediates of transcription-coupled repair have been isolated so far, it is believed that this pathway leads to formation of a $UvrA_2B$–DNA complex, converging with the global repair pathway described above.

One of the fundamental questions concerning NER is how a single repair system recognizes and processes modifications of different sizes and with different chemical properties whose only common property seems to be that they are modifications of the standard nucleotides found in undamaged DNA (Table 1). It has been proposed that the multi-step mechanism results in higher specificity of damage recognition [16,17]. If early steps of recognition identify features similar to a lesion, but later steps do not confirm that a proper substrate is present, $UvrA_2B$ dissociates from the DNA. In this view, the UvrB–DNA pre-incision complex is a key intermediate because once it is formed, dual incision will take place. The faithful discrimination between damaged and undamaged DNA is crucial to avoid spurious repair, which interferes with vital DNA-dependent processes and may introduce mutations through error-prone repair synthesis.

Functional domains of the UvrABC proteins, which are highly conserved among bacteria, have been proposed based on sequence motifs and mutagenesis studies [18]. The sequence of UvrB is related to helicases of superfamilies I and II, as shown by six helicase sequence motifs that are distributed over the first 544 residues of the 673 residue protein (residue numbers refer to the *Escherichia coli* protein). UvrB does not possess helicase activity, but the $UvrA_2B$ complex displays helicase-like activity [19]. UvrB mutations that cause a defect in this activity are also defective in NER [20]. The C-terminal residues of UvrB, which share homology with UvrC, interact with both UvrC and UvrA. Residues 115–250 of UvrB share homology to the Mfd protein; presumably, both UvrB and Mfd interact with UvrA through these homologous residues.

Great advances in understanding the molecular details of UvrABC-mediated DNA repair have been made. However, while structural information for other repair systems such as photolyase has been available (reviews in this special issue), no structures of NER components had been solved until recently. Now, four structures of the bacterial NER component UvrB have been independently determined: (1) two structures of UvrB from *Thermus thermophilus* [21,22]; (2) UvrB from *Bacillus caldotenax* [23]; and (3) a C-terminal fragment of UvrB from *E. coli* [24]. This review will focus on these three-dimensional structures. In addition, it will discuss recent biochemical data not included in previous reviews [17,18,25–27] and revisit data on UvrB mutants in light of the structural data now available.

2. Structure of UvrB

In this review, reference will be made to crystal structures of UvrB from *T. thermophilus* [21,22] (PDB codes 1C4O and 1D2M, respectively), solved at a resolution of 1.9 Å (recently improved to 1.5 Å, M.M., unpublished), and of UvrB from *B. caldotenax*, solved with and without bound ATP at a resolution of 3.0 and 2.6 Å [23] (PDB codes 1D9Z and

1D9X, respectively). UvrB proteins from *E. coli*, *T. thermophilus* and *B. caldotenax* will be designated as ecUvrB, ttUvrB and bcUvrB, respectively. Residue numbers refer to bcUvrB if not stated otherwise.

The UvrB molecule consists of five domains, which are referred to as 1a, 1b, 2, 3 and 4. The structure of bcUvrB in complex with ATP is shown in Fig. 1b to illustrate the overall architecture of the

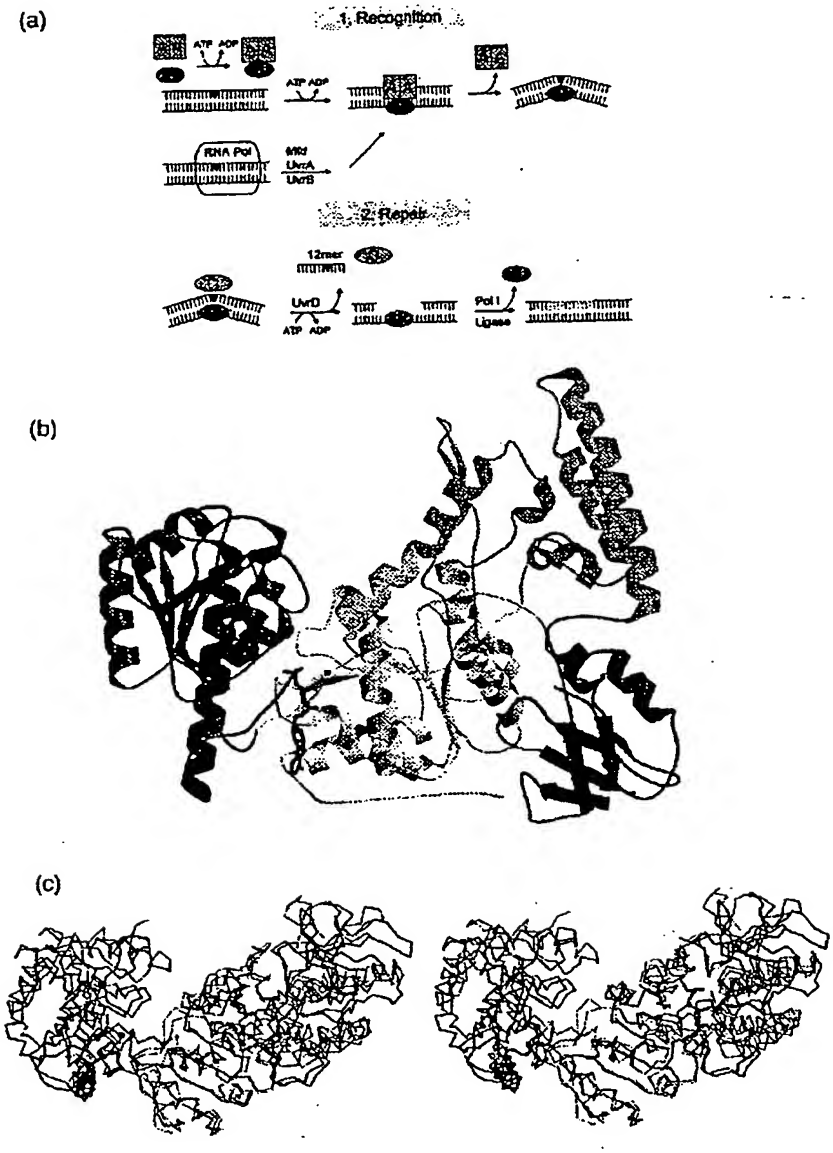

protein. Domain 4, disordered in both the bcUvrB and the ttUvrB crystal structures, is missing in the models. The structure of a UvrB fragment containing this C-terminal domain has been studied by both X-ray crystallography [24] (PDB code 1QOJ) and NMR spectroscopy [28] (see Section 4). Domain 2 is partially disordered to various degrees. In contrast, domains 1a, 1b, and 3 are well defined in both the bcUvrB and the ttUvrB crystal structures.

The helicase motifs are distributed among domains 1a and 3. Connected to each other by a single short linker, these domains both adopt an $\alpha/\beta/\alpha$ sandwich-fold. The ATP binding site is located at the interface between domains 1a and 3. The sequence similarity of UvrB (residues 114–251) with the Mfd protein spans parts of domain 1a and all of domain 2. The latter consists of anti-parallel β-strands and two α-helices. Domain 1b consists of two mainly α-helical polypeptide stretches that both connect to domain 1a. The 1a/1b nomenclature was chosen because domain 1b is neither completely independent, nor an integral part of domain 1a. A flexible β-hairpin (residues 90 to 115) extrudes from domain 1a; its tip forms hydrophobic and ionic contacts with residues in domain 1b, thereby bridging a cleft between domains 1a and 1b. Domain boundaries for the structures of ttUvrB were chosen slightly differently (Table 2).

The two independently solved structures of ttUvrB are almost identical within experimental error, with an rms deviation of 0.24 Å for 511 superimposed Cα coordinates. This is to be expected since the same enzyme was crystallized similarly, based on conditions initially described by Shibata et al. [29]. Crystallized under different conditions (using PEG instead of Li_2SO_4 as a precipitant [23]), bcUvrB is present in a distinct crystal packing. Furthermore, the amino acid sequences of bcUvrB and ttUvrB differ. Nevertheless, the structures are quite similar (Fig. 1c). The rms differences are 0.8 Å for 175 superimposed Cα positions in domain 3, and 1.3 Å for 325 superimposed Cα positions in the remainder of the molecule. Most biochemical studies have been performed with ecUvrB and not with ttUvrB or bcUvrB. Because the degree of sequence conservation among the three enzymes is high (~60% pairwise sequence identity), we expect the structure of ecUvrB to be very similar to the structures of bcUvrB and ttUvrB. Moreover, bcUvrB complements ecUvrA and ecUvrC in an in vitro incision reaction (M.S. and B.V.H., unpublished). Consequently, the biochemical results that have been obtained for ecUvrB may confidently be interpreted in the context of the bcUvrB and ttUvrB structures. While the fold and conformation of the domains of ttUvrB and bcUvrB are highly similar, there are significant differences in domain orientation (discussed in Sections 3 and 6).

The classification of UvrB as a member of the helicase superfamily II, which is based on six stretches of conserved amino acid residues [30], suggests possible similarities in the three-dimensional structures of these enzymes. Indeed, a comparison of the UvrB structure with all known structures using the program DALI [31] shows that a member of the helicase superfamily II, the RNA–helicase NS3 from hepatitis C virus [32], is the closest structural neighbor of UvrB. The structural similarity to helicases of both superfamily I and II extends beyond the heli-

Fig. 1. (a) Recognition and repair of damaged DNA by UvrABC. (top) In the global repair pathway, UvrA and UvrB form a hetero-trimer that directly recognizes damaged DNA. In the transcription coupled repair pathway, the Mfd protein recruits UvrA to damaged DNA bound to a stalled RNA polymerase. Both pathways lead to the formation of the UvrB–DNA pre-incision complex after dissociation of UvrA. (bottom) UvrC binds to the pre-incision complex and cleaves the DNA on both the 3′ and 5′ side of the damage. UvrD removes the incised oligonucleotide and UvrC, while UvrB remains bound to the gapped DNA until polymerase I fills the gap. (b) The structure of bcUvrB in complex with Mg^{2+}–ATP. Domains 1a, 1b, 2 and 3 are shown in yellow, green, blue and red, respectively. The β-hairpin bridging the gap between domains 1a and 1b is shown in cyan. The ATP molecule bound at the interface between domains 1 and 3 is indicated. Figures of the structures were made with Molscript [65] and Raster3D [66] if not stated otherwise. (c) Domain orientation in bcUvrB and ttUvrB (1D2M). View from the bottom relative to the view in (b). Domains 1a of each molecule have been superimposed, indicating different orientations of domain 3 relative to domain 1a in the two models. As a consequence, the ATP binding site is more accessible in bcUvrB than in ttUvrB. Both molecules are shown as Cα traces, with ttUvrB in gray and bcUvrB color coded as in (b). Superposition of domains 3 of bcUvrB and ttUvrB would require a rotation about an axis passing near Pro 414, which is indicated by a red sphere.

Table 2
Structural domains of UvrB

Domain	Residues	Motifs	Fold	Interacts with	1C40	1D2M
1a	1–89,116–150, 324–346, 379–411	I, Ia, II, III	α/β/α	ATP	H1	1A
β-hairpin	90–115		β-hairpin	ssDNA?	P1 (A1)	α-domain
1b	252–323, 347–378		α	ssDNA?, dsDNA?	P1 (A2, A3)	α-domain
2	151–251		mainly β	UvrA	P2	β-domain
3	412–595	IV, IVa, V, VI	α/β/α	ATP, dsDNA?	H2	2A
4	ec628–ec673		2 α-helices	UvrA, UvrC	C	C-terminal

Motifs refers to presence of helicase superfamily I and II motifs as defined by Gorbalenya et al. [30]. Columns labeled 1C4O and 1D2M give the alternative domain names chosen for the tUvrB structures [21,22].

case motifs to encompass most of domains 1a and 3. Fig. 2 illustrates that the structures of UvrB and those of the helicases PcrA, Rep and NS3 [32–34] share a core structure of helicase motif-containing loops and parallel β-strands whose connectivity is preserved. Superposition of the PcrA and NS3 structures revealed that the respective helicase motifs IV of superfamily I and II do not align. Therefore, motif IV of superfamily II was renamed to IVa to distinguish the two [32,35]. Although UvrB belongs to superfamily II and contains motif IVa, it additionally shares motif IV with the superfamily I helicase PcrA. This motif connects the two helicase-domains; its absence in NS3 results in a connection between the domains different from that observed in UvrB and PcrA. Furthermore, UvrB contains an N-terminal α-helix, involved in ATP binding, that is present in PcrA and lacking in NS3. On the other hand, the

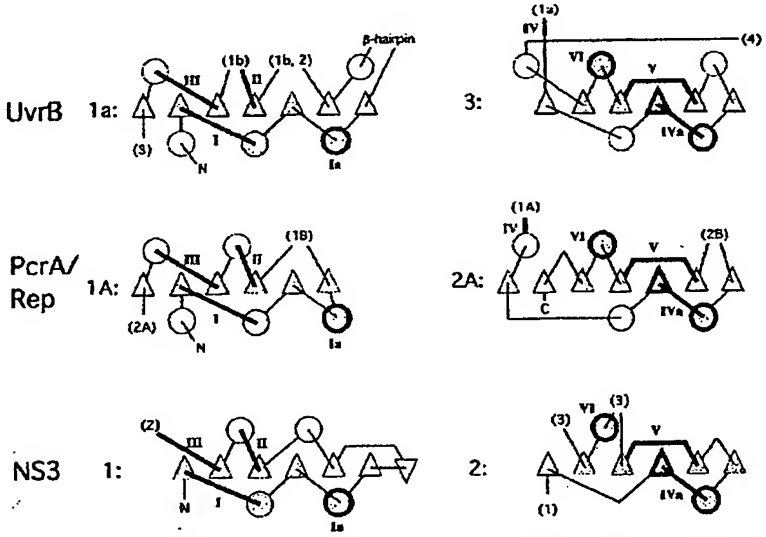

Fig. 2. Common secondary structure elements in domains 1a and 3 of UvrB and in helicase domains [32–34]. β-strands are shown as triangles (tips pointing in the same direction indicate parallel sheets), α-helices as circles, loops as lines. Helicase motifs are labeled by roman numbers and indicated by thick lines. The common core of each domain is shaded. Numbers in parentheses indicate connections to other domains.

similarity in sequence at the domain interface (including motifs II, III, and V) and in the orientation of the two domains is highest between NS3 and UvrB, in accordance with their common classification into helicase superfamily II. A feature unique to UvrB is the C-terminal α-helix of domain 3 (Fig. 2) and the following loop that tethers the disordered domain 4 near the domain interface in the three-dimensional structure.

Similar to helicases, ecUvrB in complex with UvrA displays an ATPase activity that is stimulated by DNA-binding [36,37]. In helicases, however, ATP hydrolysis is coupled to strand separation, while in the $UvrA_2B$–DNA complex, it is coupled to damage recognition and formation of the pre-incision complex. In addition, $UvrA_2B$ shows a limited helicase-activity both on undamaged and damaged DNA [19,38]. It is not clear if this helicase activity is limited because (1) $UvrA_2B$ has no translocation activity at all, (2) $UvrA_2B$ has low processivity, or (3) the strands separated by $UvrA_2B$ re-anneal after $UvrA_2B$ has passed. Moreover, it is not clear which role, if any, the helicase-like activity of $UvrA_2B$ plays in the NER mechanism. Roles in translocating to the damaged DNA or in recognizing the damage have been suggested, but the available data is still inconclusive.

Apart from the structural similarities to helicase and related ATP-hydrolyzing enzymes, UvrB has no other known structural neighbors. In particular, there is no structural similarity to the repair protein AlkA (see 'Structural studies of human alkyladenine glycosylase and *E. coli* 3-methyladenine glycosylase' by T. Ellenberger in this special issue), in spite of a limited sequence identity between the two proteins that was noted in the past [18].

3. ATP binding and hydrolysis coupled to domain motion

UvrB's ATP binding site is located between domains 1a and 3. The structural similarity of these domains to helicase domains suggests similarity in the function of ATP binding and hydrolysis. Structures of helicases in the presence and absence of cofactor and/or DNA show distinct orientations of the two domains that bind ATP, indicating that translocation is coupled to ATP hydrolysis by these domain motions. The role of the helicase motifs in this process has been studied in detail [39]. Motifs I and II correspond to the Walker A and B motifs found in many ATPases [40]. Glycine residues of motif I bind the phosphate moiety of ATP. An aspartate and glutamate (in motif II) bind to Mg^{2+} and activate the water molecule that initiates hydrolysis. In the ATP-free form, the conserved lysine of motif I replaces the Mg^{2+}, while in the ATP-complex, this residue interacts with the γ-phosphate. In the second domain, two arginines (both in motif VI in superfamily II, and one each in motif IV and VI in superfamily I) are located near the scissile P–O bond during catalysis. These residues are believed to polarize the scissile bond and to stabilize the developing negative charge at the β-phosphate during ATP hydrolysis. The other motifs are not directly involved in ATP hydrolysis, but rather have a role in DNA-binding and coupling ATP hydrolysis to strand separation [39].

The ATPase activity of UvrB differs from that of helicases. The *E. coli* enzyme is almost inactive unless truncated at its C-terminus or in complex with UvrA. In these cases, the ATPase is readily detectable and is stimulated by DNA [36,37]. In contrast to ecUvrB, ttUvrB by itself displays ATPase activity. Not further activated by truncation of the C-terminal domain, it is less stimulated by ssDNA in comparison to ecUvrB [22,41]. Stimulation of ecUvrB's ATPase by ssDNA is due mainly to changes in k_{cat} rather than K_M [37,42]. The rather low affinity of UvrB for ATP ($K_M = 1$–2 mM) is increased in complex with damaged dsDNA ($K_D <$ 10 μM) [9]. Contrary to UvrA, which hydrolyzes both GTP and ATP, UvrB is specific for ATP [37].

ATP hydrolysis in the $UvrA_2B$–DNA complex is coupled to damage recognition and formation of the pre-incision complex. ATPase-deficient mutants of UvrB (Table 3) are deficient in repair and associated supercoiling activity as well as in the limited strand separating activity [36,43–45]. Investigating the role of UvrB's ATPase activity in the $UvrA_2B$–DNA complex is complicated by UvrA's ATPase activity. While the role of UvrB's ATPase activity prior to dissociation of UvrA is still uncertain, its role after formation of the UvrB–DNA complex is known in detail. When bound ATP is removed from the UvrB–DNA pre-incision complex, no incision takes

Table 3
Mutants of *E. coli* UvrB. Roman numerals in column 'Domain' refer to helicase motifs. n.r.: not reported, TT: thymine dimer. B in the column 'DNA complexes' refers to formation of the pre-incision complex as demonstrated by footprinting experiments, AB to the $UvrA_2B$–DNA complex and BC to the UvrBC–DNA complex

Mutation	Domain	UV survival	ATPase	DNA complexes	Incision	References
none		normal	in AB complex	AB, B, BC	3′, then 5′	[18,25–27,71]
K45A	1a (I)	reduced	none	AB, no B	none	[20]
G39S/D, G44R	1a (I)	reduced	n.r.	n.r.	n.r.	[45]
R544H, R541H + E514K	3 (VI)	reduced	none	AB, no B	none	[45]
D511A	3 (V)	reduced	reduced	no B	none	[60]
D338A	1a (II)	reduced	none	no B	both reduced to < 5%	[60]
E514K	3	reduced	normal	reduced B	reduced to 50%	[45]
G509S	3 (V)	reduced	reduced	no B	none	[45]
D479A	3	reduced	enhanced	B	3′ reduced, 5′ normal	[60]
F652L	4	reduced	normal	B, no BC	3′ impaired, 5′ normal	[52]
574Δ, 630Δ, 649Δ	4	reduced	n.r.	B, no BC	3′ impaired, 5′ normal	[51]
609Δ (UvrB*)	4	reduced	A-independent	B, no BC	3′ impaired, 5′ normal	[51]
E99A,	β-hairpin,	n.r.	n.r.	no B, interferes with	3′, no 5′	[50]
E266A, E399A	1b	n.r.	n.r.	ssDNA binding	3′, no 5′	[50]
F366W,	1b,	normal	n.r.	contacts TT in ssDNA	n.r.	[50]
F497W	3 (V)	normal	n.r.	contacts TT in ssDNA	n.r.	[50]
F188W	2	normal	n.r.	quenched by ssDNA	n.r.	[50]

place, but UvrC is still able to bind [9]. Addition of ATP or ATPγS restores both 3′ and 5′ incision activities. Presumably, ATP binding changes the conformation of both UvrB and DNA in a way required for 3′ incision [46]. Addition of ADP instead of ATP does not promote 3′ incision. For the 5′ incision, however, it is sufficient to add ADP, as was demonstrated with 3′ pre-nicked DNA substrates [46,47]. In a study analyzing the effects of DNA flanking the lesion, Moolenaar et al. [48] have discovered DNA substrates that specifically bind to UvrB in the absence of UvrA (Table 4). No cofactor is required for the formation of these complexes or subsequent binding of UvrC. However, UvrC does not catalyze 3′ incision unless ATP is added. Addition of ATPγS is not sufficient, indicating that ATP hydrolysis by UvrB occurs in absence of UvrA in this special case. Taken together, these data suggest that ATP hydrolysis by UvrB followed by binding of a new molecule of ATP is necessary to present the damaged DNA to UvrC for 3′ incision [46].

3.1. Structure of the ATP binding site

The structure of ATP-bound UvrB has been obtained by soaking bcUvrB crystals in Mg^{2+}-ATP [23] (PDB code 1D9Z). Similar experiments with the ttUvrB crystals, which contain a sulfate molecule from the crystallization buffer in the ATP binding site, have not yielded cofactor-bound ttUvrB [21]. The ATP concentration used was higher than that necessary for binding of fluorescent ATP or ADP analogues in solution. Presumably, the domain orientation present in the crystals prevented binding of ATP [21].

The ATP-molecule is bound to bcUvrB mainly at the adenine and phosphate moieties (Fig. 3a). The adenine-binding pocket is formed by the side chains of Tyr 11, Gln 14, Gln 17 of domain 1a and Pro 414 of domain 3. Hydrogen bonds by Gln 17 and the main chain carbonyl of Glu12 to N6 and N7 of the adenine explain the specificity for ATP. Gln 17 is conserved throughout the UvrB sequences, and corresponds to Gln16 in the helicase PcrA, which has a similar ATP-binding pocket. In contrast, the hepatitis C helicase NS3 lacks the structural elements for this binding pocket (Fig. 2), which is in agreement with its non-specific binding to all NTPs.

Motif I (residues 32 to 48) contains the typical P-loop that is observed in many other NTP binding proteins [40]. The triphosphate moiety is bound by

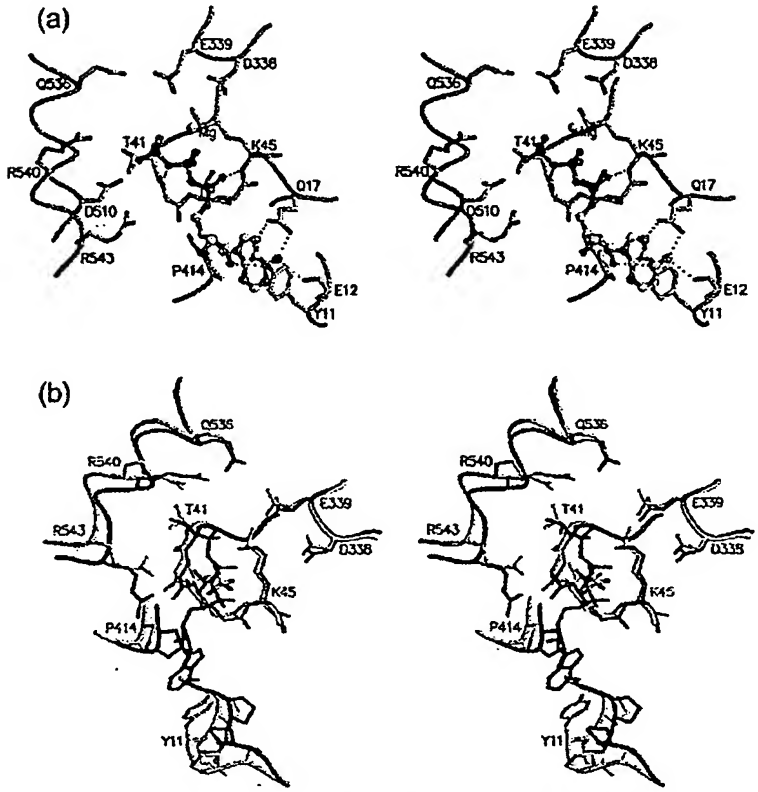

Fig. 3. The ATP binding site. (a) ATP bound to bcUvrB. Residues in the vicinity of the ATP are shown in all-bonds representation. The ATP molecule is shown as ball-and-stick model and the Mg^{2+} ion is indicated by a sphere; H-bonds are shown as dotted lines. (b) Superposition of the ATP binding sites of bcUvrB and ttUvrB (1C4O). The ATP molecule of bcUvrB is drawn in black and the sulfate molecule of ttUvrB is shown in light gray for the sulfur and dark gray for the oxygen atoms. The backbone and residues of bcUvrB are shown in light gray, those of ttUvrB in dark gray. Residue numbers refer to bcUvrB.

hydrogen bonds donated by main chain amides of residues 41 to 45. In addition, the positive charge of the side chain of Lys 45 is in close vicinity to the γ-phosphate. The Mg^{2+}-ion is bound to oxygen atoms of the triphosphate. The ion is close to the carboxylate side chains of Asp 338 and Glu 339, but does not interact directly with these residues of helicase motif II.

In the ttUvrB structure, a sulfate ion bound by residues of motif I is located roughly at the position of the β-phosphate in the bcUvrB structure (Fig. 3b). While the overall architecture of the ATP binding site is similar in bcUvrB and ttUvrB, there are differences in the adenine-binding pocket due to differences in primary sequence. ttUvrB has a deletion at bcTyr 11, and bcGln 14 is replaced by ttLys 11. While the position corresponding to Gln 14 is highly variable in different UvrB sequences, Tyr 11 is type-conserved (mostly either Phe or Tyr) in all sequences except that of ttUvrB. The deletion in ttUrB could be responsible for the higher basal ATPase activity in the absence of UvrA and DNA (see below).

A superposition of domains 1a of ttUvrB and bcUvrB shows that the two relative orientations of domains 1a and 3 in bcUvrB and ttUvrB are signifi-

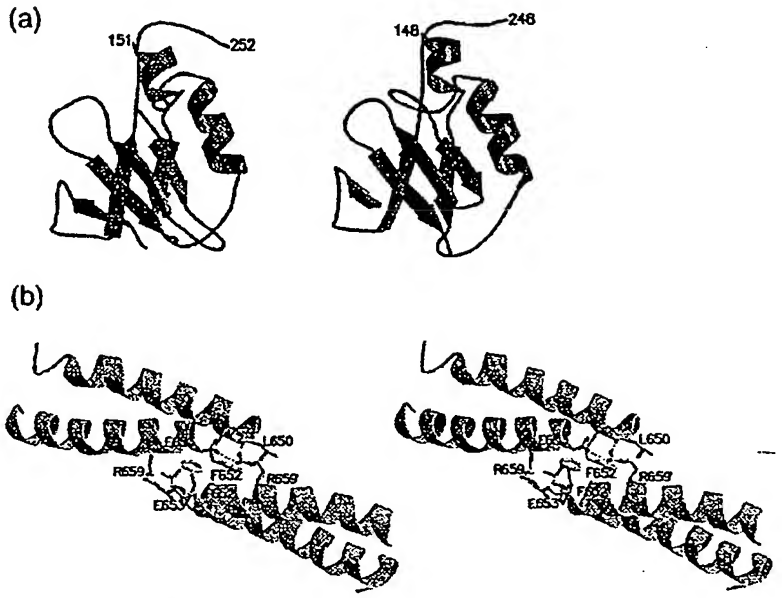

Fig. 4. Domains interacting with UvrA and UvrC. (a) Ribbon representation of domain 2 in bcUvrB (left) and ttUvrB (1D2M, right). (b) The structure of the C-terminal domain of ecUvrB shown as a dimer as observed in the crystalline state. The intermolecular salt bridge between E653 and R659 and the hydrogen bond between R659 and the main chain oxygen of L650 are indicated by dotted lines.

cantly different (Fig. 1c). The transition between the two orientations amounts to a rotation by 13° about an axis passing through Ile 412, which is located in the loop connecting the two domains. The extended conformation of this loop suggests that it can act as a hinge between the two domains. Because the individual domains superimpose well and the domain interface is identical in sequence, the difference in domain orientation is most likely due not to inherent differences between ttUvrB and bcUvrB, but rather to differences in the packing forces of the crystals. This suggests that the domain orientation is variable in solution and responds to binding of ATP or DNA, as demonstrated for PcrA [34]. As a consequence of the distinct arrangements, ttPro409 is closer to domain 1a than the corresponding bcPro414 such that the adenine-binding pocket is narrower in the ttUvrB crystals than in the bcUvrB crystals (Figs. 1c and 3b). Movement of this proline and the differences in sequence between ttUvrB and ecUvrB on the opposite side of the binding pocket (Tyr 11) might play a role both in the different basal ATPase activities of ttUvrB and ecUVrB and in the distinct effects of removal of the C-terminal domain. The loop that connects domain 3 to the disordered domain 4 is located close to Pro 414 and the ATP binding interface. Removal of domain 4 might change the conformation of this loop and increase the flexibility of the neighboring Pro 414 with respect to domain 3, thus uncoupling ATP hydrolysis and domain movement in ecUvrB. In ttUvrB, the absence of Tyr 11 from the binding pocket might render the adenine less sensitive to changes on the opposite side of the pocket caused by movement of the proline residue.

3.2. Coupling of ATPase activity to domain motions

The importance of residues from helicase motif V and VI for ATP hydrolysis has been shown by random mutagenesis of ecUvrB [45]. Although capable of binding DNA in the $UvrA_2B$ complex, UvrB is unable to hydrolyze ATP when Arg 540 or Arg

543 are mutated. The role of the arginines in motif VI has also been studied in detail for the helicase PcrA, the structure of which has been determined in complex with DNA and ATPγS [34]. In this substrate complex, the distance between the side chain Nη2 of Arg 287 and the γ-phosphate is 3.6 Å. In the bcUvrB structure, the corresponding distance to Arg 543 Nη2 is 5.8 Å. This longer distance might be a reason why ATP is not hydrolyzed by UvrB in the absence of DNA. In the case of PcrA, the protein–ATP complex and the protein–DNA–ATP complex differ in domain orientation, ATP conformation and loop conformation, all of which modulate the relative orientation of ATP and active site residues [34,49]. Similar effects might position Arg 543 (or Arg 540) of UvrB such that it stabilizes the developing negative charge at the β-phosphate during ATP hydrolysis. The overall similarity of ATP-interacting domains of UvrB, NS3 and PcrA strongly suggests that, similar to helicases, ATP hydrolysis in UvrB is coupled to domain motion.

4. Protein–protein interaction: domains 2 and 4

UvrB interacts with UvrA and UvrC in solution and in complex with DNA. The interactions are probably exclusive, as no complex containing all three proteins has ever been detected. Sequence comparisons have suggested that residues of domain 2 and 4 have a role in these protein–protein interactions [18]. Fusion proteins of maltose binding protein with either residues ec116 to ec251 or ec548 to ec674 directly show that domain 2 interacts with UvrA and domain 4 interacts with both UvrA and UvrC [50]. Mutations in or deletion of domain 4 (see Table 3) result in failure of the DNA–UvrB pre-incision complex to bind to UvrC [51–53]. However, earlier stages of damage recognition that require interactions between UvrA and UvrB are not affected [51,52,54]. Mutations or deletions in domain 2 that disrupt the interaction between UvrA and UvrB have not been characterized so far. There are no obvious candidates for such mutations because the sequence conservation in this domain is low (only four residues, Pro 151, Phe 193, Gly 197 and Arg 213 are strictly conserved).

The fold of domain 2, a β-sheet of four anti-parallel strands that interacts with two anti-parallel β-strands and an α-helix, is shown in Fig. 4a. The globular domain is connected to domains 1a and 1b by its N-terminus and C-terminus, respectively. No strong or extensive interactions with either of these domains are observed. The fold is reminiscent of that of ferredoxin or ubiquitin, but the structural similarities are too low to be detected by automatic methods. During structure determination of bcUvrB it was noted that the orientation of domain 2 changes relative to the remainder of the molecule when derivatized with gold or mercury compounds [23]. Likewise, a comparison of the bcUvrB and the ttUvrB structures shows a variable orientation. The quality of the electron density of domain 2 is low in all three structure determinations and decreases with distance from the connections to the ordered parts of the molecules. As a consequence, some of the loops connecting secondary structure elements could not be modeled. Parts of the domain were built as poly-alanine because the sequence assignment of these residues is uncertain. Furthermore, the crystallographic atomic displacement parameters of the residues in domain 2 are high. Because the location of the few strictly conserved residues is uncertain, the structures do not readily indicate possible UvrA-interaction sites on domain 2.

The C-terminal domain 4 is completely disordered in all three UvrB crystal structures. The primary sequence of the C-terminus shows about 60 residues of moderate conservation at the very C-terminal part, separated from domain 3 by a linker of highly variable sequence and length (24–72 residues). No structural information on the linker region or the location of the C-terminus of UvrB relative to the other domains is available. However, the conformation of the C-terminal 55 residues of ecUvrB has been studied by X-ray crystallography [24] and NMR spectroscopy [28] as a histidine-tagged fusion protein. The ordered region of the fragment (residues ec628 to ec673) adopts a helix-loop-helix conformation that is stabilized by inter-helix hydrophobic interactions. In the crystalline state, two neighboring molecules interact in a head to head fashion, with hydrophobic and ionic interactions involving side chains from the loop (Fig. 4b). It has been suggested that the interaction between UvrC and UvrB is similar to that observed between neighboring molecules in the crystal structure of the UvrB fragment [24].

This interpretation is supported by mutagenesis studies and the high conservation of most residues present at the interface formed by the head to head arrangement.

UvrA can interact with both domain 2 and domain 4 of UvrB. In the $UvrA_2B$–DNA complex, UvrA presumably binds simultaneously to these domains, possibly constraining their relative orientation. However, UvrA-binding is not expected to constrain the domain motion between domain 1a and 3, because their respective connections to domains 2 and 4 are flexible. The interaction between UvrA and domain 4 is dispensable for the formation of the pre-incision complex. Maybe the role of this interaction is to ensure the correct sequence of events by preventing UvrC from binding to the nucleoprotein complex before UvrA has dissociated.

5. DNA substrates and intermediates

UvrB does not bind to dsDNA by itself. Furthermore, its affinity for ssDNA, with or without lesions, is very low [50]. Apparently, UvrB lacks strong binding sites for either dsDNA or ssDNA. However, after UvrA-mediated formation of the pre-incision complex, the (non-covalent) UvrB–DNA interaction is quite strong, even at high ionic strength [7] or after excision of the lesion [14]. How does UvrB bind to DNA? Moreover, why does formation of the UvrB–DNA complex require UvrA? The nucleoprotein complexes formed by UvrA, UvrB and/or UvrC with several nicked, truncated and mismatch-containing DNA constructs have been studied to address these questions (Table 4).

The affinity of UvrA for damaged DNA is $\sim 10^3$-fold higher than that for undamaged DNA [55]. The discrimination factor achieved by UvrA and UvrB together is much higher. Furthermore, UvrA binds preferentially not only to DNA structures that are substrates for NER, but also to mismatch-containing and thus partially unpaired DNA that is not repaired by NER [56]. These results support the view that a lesion has to pass different checkpoints in several stages of recognition, and that the nucleoprotein complex will dissociate if any one of these tests fails. Early stages of recognition may be by-passed with artificial substrates that resemble the DNA-conformation present at a later stage of recognition. For example, recent studies show that unmodified mismatch-containing DNA that is pre-nicked at the 3′ side of the lesion ("flap" substrate) is cleaved by UvrBC, even in the absence of UvrA [47]. Furthermore, damaged DNA containing 10 or more consecutive mismatches is incised at the 5′ side, but not at the 3′ side of the lesion [57]. The observation that the 5′-incision is uncoupled from the 3′ incision with these special substrates suggests that the presence of single stranded DNA at the 3′ side triggers 5′ incision. This notion is supported by earlier observations of additional incisions 5′ to the 5′-incision site at high UvrB concentrations [53], and damage-independent hydrolysis 5′ of single strand/double strand junctions [58].

The effects of unpaired DNA on UvrA-dependent and UvrA-independent endonuclease activity of UvrBC have been studied systematically [57]. If the modified base is part of a bubble of 3–6 mismatched bases, UvrA-independent damage-specific 3′ and 5′ incision by the UvrBC nuclease occurs. An increase of the size of the bubble to eight mismatches causes the level of UvrA-independent incision to drop sharply, whereas further increase in the number of mismatches leads to uncoupled 5′ incision. These and earlier studies [16, 47] indicate that the DNA in the preincision complex is not extensively unwound.

In a complementary approach, Moolenaar et al. studied the role of DNA flanking the lesion [48]. The flanking DNA was modified either by introducing nicks at the 3′ or 5′ incision sites of UvrABC on the damaged or the opposite strand, or by truncating one or both strands at these positions (Table 4). Truncating both strands at the 3′ incision site does not inhibit formation of UvrB–DNA or UvrB–UvrC–DNA complexes in the presence of UvrA. Truncation at the 5′ incision site, however, prevents loading of UvrB and UvrC on DNA. The authors conclude that UvrA approaches the damage in an asymmetric manner from the 5′ side (referring to the damaged strand). Surprisingly, UvrB alone binds in a damage-dependent manner to substrates truncated on the 5′ side of the damage leading to a stable pre-incision complex. If only the undamaged strand is truncated opposite to the 5′ incision site, 3′ and 5′ incisions are observed at the expected sites. This is

Table 4
Intermediates and products formed by UvABC and various DNA constructs

DNA construct		Intermediates and products formed in presence of UvrA	without UvrA	References
dsDNA with lesion		A AB B BC 3' 5'	-	[18, 25-27, 71]
mismatches				
3-6 bp		A AB B BC 3' 5'	3' 5'	[16, 57]
8 bp		A AB B BC 3' 5'	-	[57]
> 8 bp		A AB B BC 5'	5'	[47, 57]
truncations				
opposite strand at 3' site		A AB B BC	-	[48]
both strands at 3' site		A AB B BC	-	[48]
damaged strand at 3' site		A AB B BC 5'	-	[48]
both strands at 5' site		A AB	B (BC)	[48]
damaged strand at 5' site		A AB	(B)	[48]
opposite strand at 5' site		A AB (B BC 3' 5')[1]	B BC 3' (5')	[48]
nicks				
3'-pre-nicked		A AB B BC 5'	-	[47, 48, 51, 52]
5'-pre-nicked		A AB	-	[48]
opposite 3' incision site		A AB B BC	-	[48]
opposite 5' incision site		A AB B BC 3' 5'	(3') 5'	[48]
dsDNA, no lesion		(A)	-	[8, 55]
5' overhanging end		(A)	BC 5'	[58], [53]
3' overhanging end		(A)	-	[53]
10 bp mismatched		A AB	-	[56]
mismatched, pre-nicked		(A)	BC 5'	[47]
ssDNA with lesion		-	(B)	[50]
ssDNA, no lesion		-	((B))	[50]

A, AB, B, BC refers to the formation of different specific nucleoprotein complexes containing UvrA/UvrB/UvrC as demonstrated in gel shift or footprinting experiments. 3' and 5' refers to incision products detected after the reaction. [1]UvrA probably does not participate in the formation of these complexes, which also form in the absence of UvrA (see following column).

the first demonstration that UvrB by itself can bind specifically to damaged DNA. Apparently, UvrB contains a damage-sensing DNA binding site. The data also show that dsDNA flanking the 5' incision site somehow presents a barrier for the formation of the UvrB–DNA pre-incision complex. This barrier can either be overcome by the ATP-dependent action of UvrA, or is removed in the truncated DNA substrates.

The effect of a nick in the strand opposite of the 3' incision site [48] provides insight into the role of ATP binding by UvrB. According to gel shift assays performed in the presence of UvrA and ATP, the nicked substrate forms a UvrB–UvrC-complex whose stability is comparable to substrates without nicks. If ATP is omitted, the presence of the nick stabilizes the UvrB–UvrC complex. However, 3' incision of the nicked substrate is very low. This can be explained in terms of two consecutive conformational changes triggered by ATP hydrolysis and subsequent ATP binding, which lead to a pro-pre-incision complex and to the pre-incision complex, respectively. If the DNA at the 3' incision site is required to go through different strained conformations in this process, introduction of a nick might stabilize the UvrB–UvrC complex and inhibit 3' incision by releasing this strain [48].

The properties of DNA substrates containing mismatches, nicks or truncated strands suggest that UvrB binds in part to single stranded and in part to double

stranded DNA in the pre-incision complex. The three-dimensional structure of UvrB provides clues as to where such single and double stranded DNA binding sites might be located.

6. DNA binding sites on UvrB

The shape of the UvrB molecule provides first insights into the location of possible DNA-binding sites. While the side of UvrB containing the ATP-binding site contains clefts and pockets, the reverse side is almost featureless. Indeed, almost all notable features concerning charge distribution, sequence conservation, distribution of structural elements and location of mutations with altered functionality are on the side of the molecule facing the viewer in Fig. 1b.

6.1. Superposition of UvrB with helicase/DNA-complexes

Provided that UvrB has a similar strand translocation mechanism as helicases of superfamilies I and II, a superposition of the helicase/DNA-complexes with UvrB might reveal the path of the translocated strand on the surface of UvrB. It could also point to structural features in UvrB that are important for the interaction with bases or with the backbone of DNA. There are three UvrB-related helicases whose structures have been determined in complex with DNA: NS3, PcrA and Rep [32–34] (Fig. 5). In all three structures, the domain corresponding to domain 3 in UvrB binds the 5′ end, and the ATP-binding domain binds the 3′ end. The DNA is bound deeply inside the respective molecules. Aromatic or aliphatic side chains located in both domains bind to DNA through stacking interactions or by intercalation. In the case of the Rep and PcrA helicases, additional domains above the single strand prevent re-annealing of the separated DNA duplex. Homology-modeling of the UvrB–DNA interaction in the pre-incision complex based on the helicase–DNA complexes places the β-hairpin of UvrB such that it obstructs the path of the DNA. There is, however, a passageway under the β-hairpin that could accommodate a single strand of DNA. This feature, which is not observed in the helicase structures, has been suggested to play an important part in the NER mechanism [21,23] as discussed below.

6.2. Surface charges and conserved residues

Protein surfaces interacting with the negatively charged backbone of DNA are expected to have a complementary positive charge distribution. Electrostatic calculations show that the largest charged surface patches are in domain 1a (negative) and domain 3 (positive) near the ATP binding site. It has been proposed that binding and hydrolysis of ATP modulates the electrostatic interactions to cause domain motion [23]. As discussed above, the structures of UvrB strongly suggest that in order for ATP hydrolysis to occur the two domains have to move closer to each other, making the interface largely unavailable for DNA binding. In addition to these large charged surface patches, there are smaller patches of positive charge at the top of domain 3 (referring to the orientation shown in Fig. 1b) and at the bottom of the cleft between domains 1a and 1b.

Conserved residues of UvrB are clustered in two regions (Fig. 5). The first cluster surrounds the ATP binding site, with conserved residues in both domains 1a and 3. This cluster is located in the part of the molecule that shares structural similarity with helicases. The second cluster is located in the β-hairpin and the surrounding region. Remarkably, many of the surface-exposed residues in the β-hairpin are highly conserved (Fig. 6). In addition to these two clusters, there are smaller patches of conserved surface residues in domain 1a (residues 66–68, 84–95) and domain 3 (residues 453–459, 474–478).

6.3. The β-hairpin

The high sequence conservation of the flexible β-hairpin and surrounding regions is not due to obvious structural constraints and thus points to a functional importance. The β-hairpin as observed in the bcUvrB structure is shown in Fig. 7a. The tip of the β-hairpin interacts with domain 1b through hydrophobic interactions (Tyr 101, Tyr 108 with Leu 361, Phe 366). Two salt bridges, between Glu 99 and Arg 367 and between Lys 111 and Glu 307, are observed in bcUvrB. The bridging residues Tyr 92–Glu 99 and Asp 112–Asn 116 are solvent exposed.

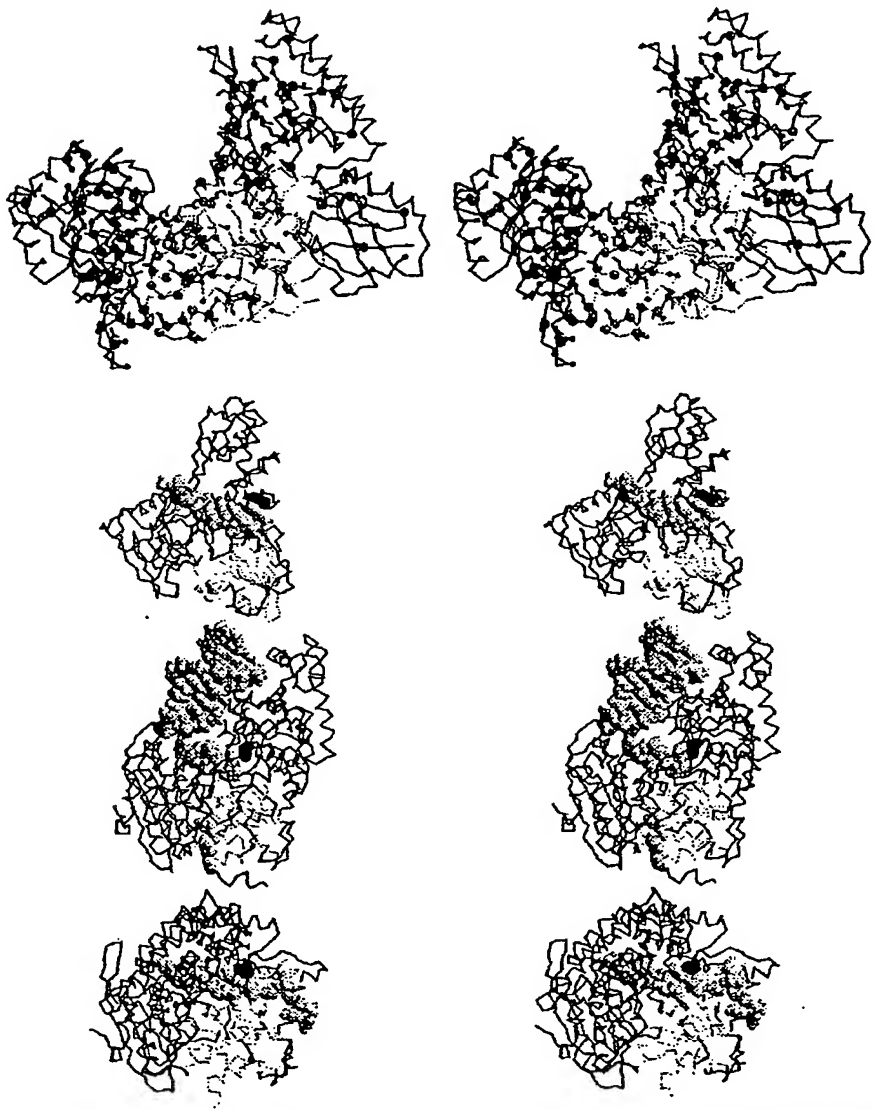

Fig. 5. (Top) Conserved residues of UvrB. View of bcUvrB as in Fig. 1b. Strictly conserved residues are shown as big spheres with the side chain in all-bonds representation. Type conserved residues are indicated by small spheres. The residue assignment in domain 2 is tentative. (bottom) Superfamily I and II helicases in complex with DNA. NS3, PcrA and Rep are shown as Cα traces, with the ATP, sulfate and DNA as light gray and intercalating residues as black cpk models. Regions in the helicase domains of NS3, PcrA and Rep that superimpose well with domain 1a and 3 of UvrB are colored yellow and red, respectively. The ATP-binding domain (corresponding to domain 1a of UvrB) is oriented as in the UvrB molecule at the top.

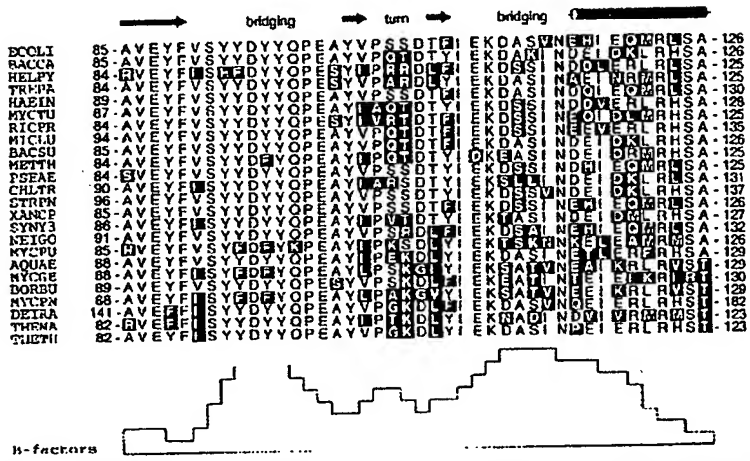

Fig. 6. Sequence conservation in the β-hairpin. The alignment of 21 UvrB proteins from different species was generated with the programs ClustalW and ALSCRIPT [67,68]. Secondary structure elements are indicated. At each position, residues other than the most frequently observed amino acid are highlighted. Main-chain B-factors of the ttUvrB structure [1C40] vary from 28 to 42 Å^2 and are shown as a histogram. Abbreviations for the different organisms are as in the SWISS-PROT database [69].

A comparison of the β-hairpin in bcUvrB with that of ttUvrB shows that the local structure of the β-hairpin tip interacting with residues of domain 1b is preserved. However, the distance between the base and the tip of the β-hairpin is different in the two molecules. Specifically, there are differences in the conformation of the bridging stretches of the β-hairpin and of several loops of domain 1b (Fig. 7b). This suggests that the size of the passageway between the β-hairpin and domains 1a and 1b is variable to a certain degree. Inspection of the atomic displacement parameters of UvrB shows high values for the bridging residues indicative of increased flexibility in this region (Fig. 6, bottom).

β-Hairpins with highly conserved hydrophobic residues have been observed both in PcrA helicase and T7 RNA polymerase, in which they have a common structural role in opening up the double strand (Fig. 8). In the case of T7 RNA polymerase, this takes place at the opening side of the transcription bubble. In both cases, the loops reach in between the two separated strands and stack with the bases located at the ssDNA/dsDNA junction. In contrast to these loops, the β-hairpin of UvrB con-

Fig. 7. The β-hairpin and its proposed role in binding to DNA. (a) Cα-trace of the β-hairpin of bcUvrB (cyan) and neighboring residues of domain 1b (green) and 1a (yellow). View from the left relative to the view in Fig. 1b. Selected residues are shown in all-bonds representation. Salt bridges are indicated by gray dotted lines. (b) Structural differences in the β-hairpin in bcUvrB and ttUvrB (1C4O). Superposition as in Fig. 1c. Both structures are shown as Cα-traces, domains 2 and 3 are omitted for clarity. Regions where significant structural differences were observed are shown in magenta. Spheres indicate positions of insertions/deletions between bcUvrB and ttUvrB, or prolines present in only one of the two proteins. (c) Hypothetical model of the UvrB DNA pre-incision complex. Surface representation of UvrB with a domain orientation derived from the superposition with the NS3–DNA complex. Domains 1b and 3 are indicated. The proposed conformation of DNA is shown as phosphate backbone in red with the undisrupted base pairs shown as spokes. Residues Tyr 146 and Phe 527 are shown in blue and the β-hairpin is depicted in cyan. (c) was made with GRASP [70].

tains conserved aromatic residues that might stack with bases not on the tip, but closer to the base of the β-hairpin. Thus, the β-hairpin in UvrB may play a role similar to that of β-hairpins in PcrA helicase and T7 RNA polymerase, but different in the structural details.

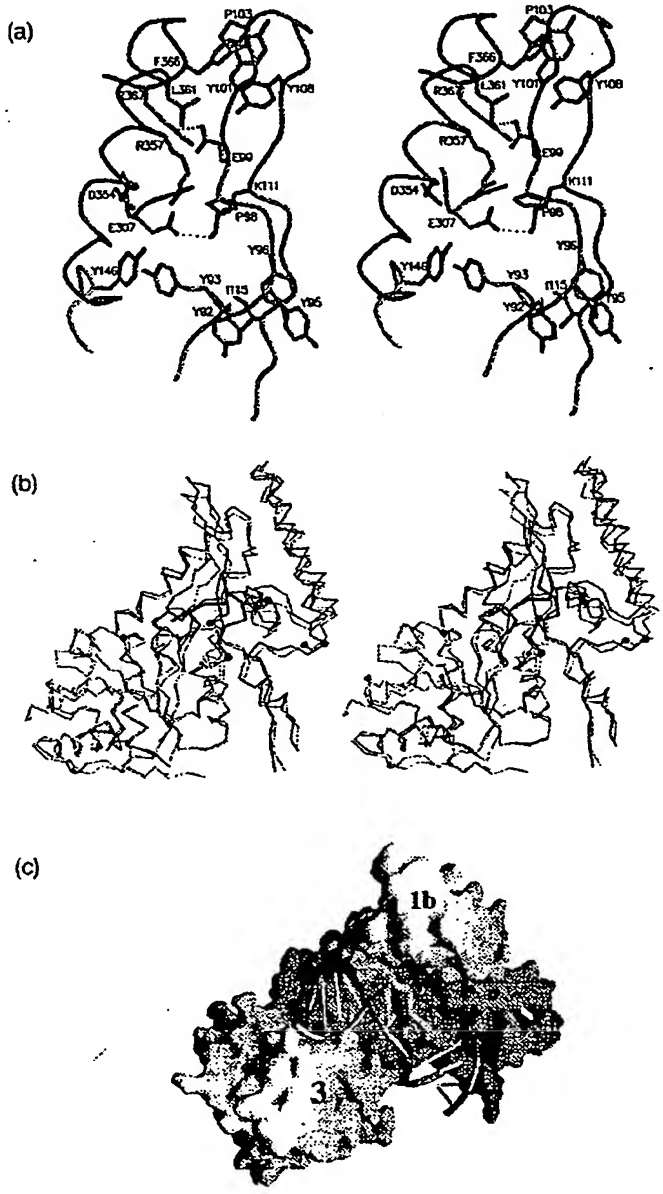

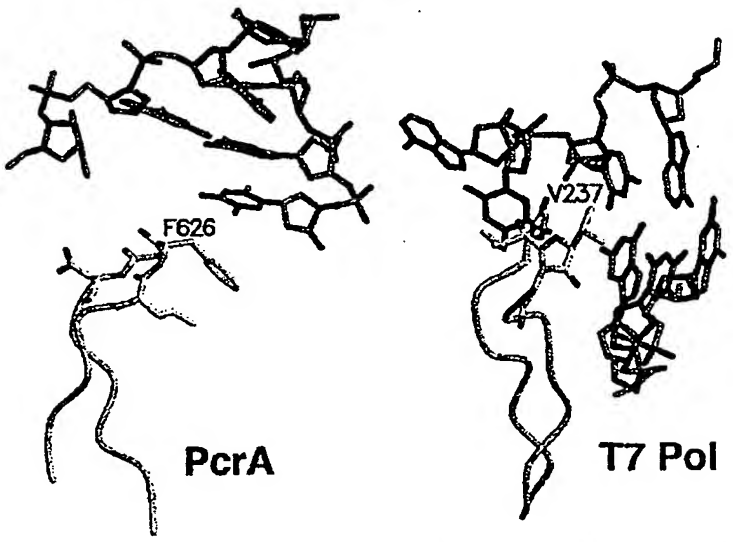

Fig. 8. Intercalating loops in PcrA helicase and T7 RNA polymerase. The loops are shown as Cα-trace. Residues that stack with DNA bases are labeled and shown in all-bonds representation.

6.4. DNA binding mutants

The effect of various UvrB mutations on UV-survival, on ATPase activity and DNA-binding has been studied [20,45,50–53,59,60]. The location of these mutations in UvrB is shown in Fig. 9; Table 3 lists those mutants that differ from wild type in their properties. One class of mutants is defective in ATPase and helicase activity, but still binds to DNA. However, because these mutants are deficient in forming the pre-incision complex they do not promote UV-resistance. A second class of mutants (ecD511A, ecG509S) shows reduced ATPase activity as well as reduced DNA binding [45,60]. However, it is not clear if the reduction in the ATPase activity is the cause or the consequence of the reduced DNA binding activity. Mutations in the C-terminal part of UvrB interfere with binding of UvrC to the pre-incision complex [51,52]. Furthermore, C-terminal deletions of ecUvrB result in UvrA-independent ATPase activity [37]. The DNA-binding properties themselves, however, are apparently not changed. Thus, no clear-cut DNA binding mutants have been demonstrated.

Studies with damaged ssDNA have shown that mutations ecF366W and ecF497W introduce tryptophan residues at locations where they photochemically split thymine dimers on the ssDNA [50]. In addition, these mutants and the mutation ecF188W show quenching of tryptophan fluorescence upon binding of ssDNA. The mutants ecE99A, ecE266A and ecE339A interfere with binding of the single stranded DNA and are deficient in 5′, but not 3′ incision [50]. Neither ATPase activity nor formation of complexes with damaged dsDNA have been reported for the latter three mutants. Therefore it is not known whether they are DNA-binding mutants or defective in another way.

7. Model for the pre-incision complex and implications for NER

Different DNA binding modes have been proposed based on the structure of UvrB. Machius et al. [21] note that cleavage of damaged DNA consistently occurs three to five phosphodiester bonds 3′

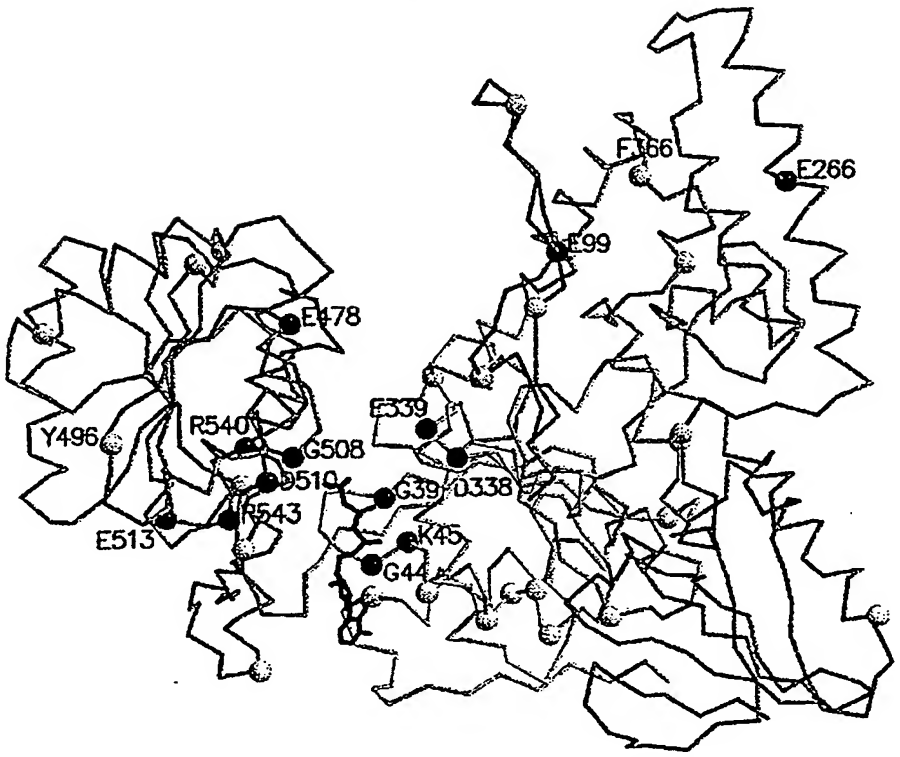

Fig. 9. Location of characterized mutations of ecUvrB (Table 3) mapped on the structure of bcUvrB. Residue numbers refer to bcUvrB and are identical to those of ecUvrB except for residues E478 (ecD479), Y496 (ecF497), G508 (ec509), D510 (ec511), E513 (ec514), R540 (ec541) and R543 (ec544). Black spheres indicate mutations with altered phenotype, light gray spheres those without.

and eight phosphodiester bonds 5′ to the lesion and conclude that the lesion is trapped at a well defined location in UvrB and then presented to UvrC. Based on the similarities with helicases, the authors propose that initially, UvrB interacts with damaged DNA such that the lesion is located above the tip of the β-hairpin. The observation that the residues ecGlu99 and ecPhe366 are critical for interaction between UvrB and damaged ssDNA [50] suggests that subsequently, the β-hairpin moves outwards, thus capturing the lesion between the β-hairpin and the two helical arms of domain 1b. The capturing mechanism is only possible if the basal region of the β-hairpin exhibits increased plasticity so that it can move away from domain 1b.

Nakagawa et al. [22] suggest a model also based on structural comparisons to helicase–DNA complexes and furthermore on the distribution of charged and conserved residues on the surface of UvrB. According to their suggestion, double stranded DNA that binds to the surface of UvrB near the β-hairpin is unwound near the interface between domain 1a and 3. One of the single strands interacts with domain 3, while the other contacts conserved residues of helicase motif Ia. The model leaves open whether the lesion is located in the single or double stranded portion of the DNA, and whether it interacts with UvrB or points outwards.

Based on a superposition of bcUvrB with the NS3 helicase–DNA complex and on the location of con-

served residues and charges on the surface of UvrB, Theis et al. [23] conclude that the β-hairpin is a binding site for ssDNA. The proposed structural model of the UvrB–DNA interaction explains why the pre-incision complex does not form spontaneously, but once formed is highly stable. The model is presented below and developed further in light of new biochemical data.

7.1. The padlock model

The hypothetical structural model of the bcUvrB DNA pre-incision complex [23] is shown in Fig. 7c. For construction of the model, domain 3 and the remainder of the UvrB model were superimposed separately with the corresponding domains in the structure of NS3 in complex with single stranded DNA. In this superposition, domain 3 is rotated towards domain 1a, thus narrowing the ATP binding site. Partially unpaired thymine-dimer-containing DNA as observed in complex with endonuclease V (PDB code 1VAS, [61]) was fitted into the model such that one strand had the same orientation as that bound to NS3. The double stranded DNA was further unwound to accommodate the β-hairpin of UvrB. Except for the domain movement, the UvrB structure in the model is identical to that observed experimentally.

The model shows that at least 5 bp of DNA have to be disrupted to insert the β-hairpin between the strands. There is sufficient space for flanking dsDNA on both sides of the β-hairpin. On one side, the double strand contacts domain 3 near helicase motif IVa; this region is positively charged, as expected for a dsDNA binding site. In close proximity to the suggested path of the DNA, the solvent-exposed aromatic residues Tyr 146 and Phe 527 might act as intercalators (Fig. 7c). The passageway between domain 1b and the β-hairpin is large enough to fit a single DNA strand without the need to disrupt the interactions observed in the crystal structure between the tip of the β-hairpin and domain 1b. The central feature of the model is that the DNA single strand is locked under the β-hairpin as long as these interactions are present and as long as the locked single stranded portion of DNA is flanked by double stranded DNA on both sides. ssDNA is incapable of forming such a stable complex with UvrB because it does not contain flanking dsDNA on both sides and thus slips through the passageway.

How is the pre-incision complex formed, and how does UvrB interact with DNA after incision? The conclusions drawn from the structural model of the pre-incision are as follows. Insertion of the β-hairpin between the two strands of duplex DNA requires a conformational change in UvrB. According to the padlock model [23], binding of UvrA (which acts as a key in the padlock analogy) is the trigger for lifting the β-hairpin away from domain 1b. In this open conformation, the helicase activity of UvrB causes $UvrA_2B$ to translocate along the undamaged strand. If no lesion is encountered for some time, the $UvrA_2B$ complex dissociates from DNA. When a lesion is encountered, UvrB resumes its original conformation upon dissociation of UvrA, thus capturing the undamaged strand and inhibiting further translocation by binding to it tightly. After incision, UvrB remains bound to the single stranded portion of the gapped duplex until polymerase I displaces it from the undamaged strand, which acts as template during repair synthesis.

7.2. A comprehensive model for UvrB's role in NER

The recent findings that UvrB binds to truncated substrates in the absence of UvrA [46,48] support the padlock model of DNA-binding. If the DNA on one side of the lesion is of limited length and single stranded, this strand can thread through the passageway under the β-hairpin without the need to disrupt intramolecular interactions of UvrB. Knowing which flanking parts of the damaged DNA are required in different intermediates allows us to expand the padlock model with respect to the location of the 3′ and 5′ incision sites relative to UvrB. Our conclusions are summarized in Fig. 10. We assume that $UvrA_2B$ approaches from the 5′ side of the lesion because a deletion of the flanking DNA on this side prevents complex formation [48]. If $UvrA_2B$ translocates along the undamaged strand, as suggested by the padlock model, the direction of translocation on this strand is 3′ to 5′. Should $UvrA_2B$ bind to a spurious DNA substrate, ATP-driven translocation would promote dissociation of $UvrA_2B$. In complex with DNA containing mono-adducts, $UvrA_2B$ translocates until UvrA dissociates when the β-hairpin reaches the

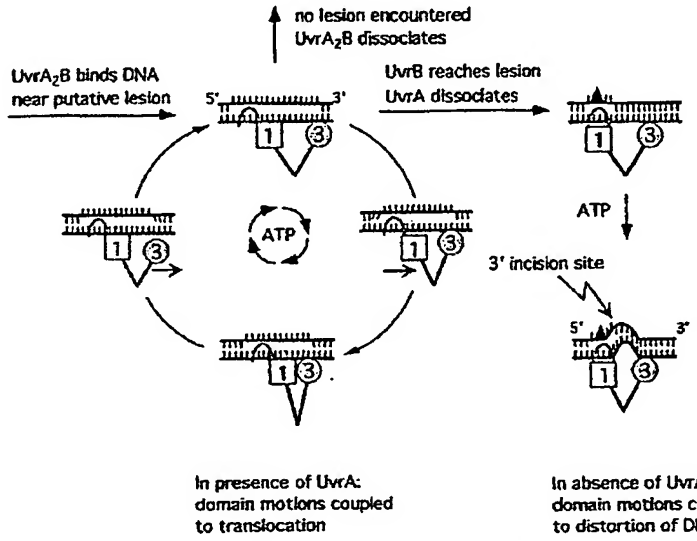

Fig. 10. Structural interpretation for the role of ATP binding and hydrolysis before and after formation of the pre-incision complex. Circles labeled "3" symbolize domain 3 and padlocks labeled "1" symbolize domains 1a/b and the β-hairpin. The padlocks are shown either closed or open, symbolizing either the conformation of the β-hairpin observed in the crystal structure or a hypothetical one in which the β-hairpin is moved away from domain 1b.

lesion. In complex with DNA with inter-strand cross-links, however, translocation of $UvrA_2B$ stops prematurely because the cross-link prevents strand separation at the lesion. Thus, the incision sites will be shifted to the 5′ side, which is indeed observed with some types of crosslinks [62].

Once UvrA has dissociated, the undamaged strand is locked. ATP-dependent domain motions will no longer be coupled to translocation, but rather will deform the locked strand in the region bound between domain 3 and the β-hairpin. It has been suggested that a strained DNA conformation is the trigger for 3′ incision [48]. Thus, we propose that the 3′ incision site is located between domain 3 and the β-hairpin as shown in the sketch in Fig. 10. The recent observation that UvrB binds to substrates truncated on the 5′ side to the lesion in the absence of UvrA [48] is in agreement with this suggestion. The 3′ side of the lesion is more important for binding than the 5′ side because it interacts with UvrB more extensively in the orientation shown in Fig. 10.

The comprehensive model of the interactions of UvrB with DNA presented here is a framework for future experiments that test its basic assumptions and the detailed predictions that can be drawn from it. Some important assumptions of the model have been made without direct evidence. For instance, it was concluded from the stability of the post-excision UvrB–DNA complex [14] that UvrB binds tightly to the non-damaged rather than the damaged strand, but this has not been demonstrated directly. This model also contradicts conclusions from earlier studies. For example, the model depicts translocation on the undamaged strand from the 5′ side of the lesion, resulting in 3′ to 5′ translocation. However, UvrB has been classified as a 5′ to 3′-acting helicase based on UvrB's preferential separation of dsDNA with 5′ overhanging ssDNA as opposed to 3′ overhanging ssDNA [63]. This preference was rationalized by 5′ to 3′ translocation of $UvrA_2B$ along the single strand presented to it at the ssDNA/dsDNA junction. However, initial binding of $UvrA_2B$ does not require such a junction and may occur anywhere on the

dsDNA. Therefore, conclusions about the helicase-like activity of $UvrA_2B$ reached with reference to the helicase substrates should be taken with caution.

8. Conclusions and outlook

The recent structure determinations of UvrB are a substantial step toward understanding the molecular mechanisms of UvrABC action. The close structural similarity to helicases strongly suggests that ATP binding and hydrolysis by UvrB are coupled to motions between the two helicase-related domains. The clear separation of UvrB into two helicase domains, two additional domains known to interact with UvrA and UvrC, and one domain proposed to interact with DNA allow interpretation of available data and design of new experiments. In particular, the structures have revealed a highly conserved patch on the surface of UvrB that includes a flexible β-hairpin representing a unique adaptation of the known core helicase architecture.

Disparate roles for the ATPase activity of UvrB have been suggested in the past. Based on similarities in sequence and function to helicases, one view is that the ATPase activity causes translocation and transient strand separation, which allow efficient location of lesions by tracking along the DNA [26,43,64]. However, UvrB's ATPase activity is not required for formation of specific complexes between $UvrA_2B$ and damaged DNA in in vitro experiments [45]. A second view, which is based on the requirement for UvrB's ATPase activity after formation of the specific complexes, suggests that this ATPase activity is important only in later stages of damage recognition [18,38]. In this view, strand separation and changes in supercoiling of DNA by $UvrA_2B$ are not attributed to a translocation mechanism, but rather to complex formation and local ATPase-dependent DNA unwinding by UvrB.

The structures presented in this review do not resolve the argument above, but rather suggest plausible mechanisms for both views. Specific experiments based on the structures and as of yet hypothetical models, combined with new structural data on UvrA and UvrC, are necessary to understand exactly how UvrABC locates lesions efficiently and distinguishes them from undamaged DNA.

Acknowledgements

The authors would like to thank Nora Goosen for sharing experimental data that were still in press, and Mark Sanderson for sharing coordinates of the C-terminal domain of UvrB.

References

[1] R.B. Setlow, W.L. Carrier, The disappearance of thymine dimers from DNA: an error-correcting mechanism, Proc. Natl. Acad. U.S.A. 51 (1964) 226–231.
[2] R.P. Boyce, P. Howard-Flanders, Release of ultra-violet light-induced thymine dimers from DNA in *E. coli* K-12, Proc. Natl. Sci. U.S.A. 51 (1964) 293–300.
[3] R.F. Hill, A radiation-sensitive mutant of *Escherichia coli*, Biochim. Biophys. Acta 30 (1958) 636–637.
[4] P. Howard-Flanders, L. Theriot, A method for selecting radiation-sensitive mutants of *Escherichia coli*, Genetics 47 (1962) 1219–1224.
[5] P. van de Putte, C.A. van Sluis, J. van Dillewijn, A. Rorsch, The location of genes controlling radiation sensitivity in *Escherichia coli*, Mutat. Res. 2 (1965) 97–100.
[6] A. Sancar, W.D. Rupp, A novel repair enzyme: UvrABC excision nuclease of *Escherichia coli* cuts a DNA strand on both sides of the damaged region, Cell 33 (1983) 249–260.
[7] D.K. Orren, A. Sancar, The (A)BC excinuclease of *Escherichia coli* has only the UvrB and UvrC subunits in the incision complex, Proc. Natl. Acad. Sci. U.S.A. 86 (1989) 5237–5241.
[8] B. Van Houten, H. Gamper, A. Sancar, J.E. Hearst, DNase I footprint of ABC excinuclease, J. Biol. Chem. 262 (1987) 13180–13187.
[9] D.K. Orren, A. Sancar, Formation and enzymatic properties of the UvrB–DNA complex, J. Biol. Chem. 265 (1990) 15796–15803.
[10] J.-J. Lin, A. Sancar, Active site of (A)BC excinuclease: I. Evidence for 5′ incision by UvrC through a catalytic site involving Asp^{399}, Asp^{438}, and His^{538} residues, J. Biol. Chem. 267 (1992) 17688–17692.
[11] E.E.A. Verhoeven, M. van Kesteren, G.F. Moolenaar, R. Visse, N. Goosen, Catalytic sites for 3′- and 5′ incision of *E. coli* excision repair are both located in UvrC, J. Biol. Chem. 275 (2000) 5120–5123.
[12] P.R. Caron, S.R. Kushner, L. Grossman, Involvement of helicase-II (UvrD gene product) and DNA Polymerase-I in excision mediated by the UvrABC protein complex, Proc. Natl. Acad. Sci. U.S.A. 82 (1985) 4925–4929.
[13] I. Husain, B.V. Houten, D.C. Thomas, M. Abdel-Monem, A. Sancar, Effect of DNA polymerase I and DNA helicase II on the turnover rate of UvrABC excision nuclease, Proc. Natl. Acad. Sci. U.S.A. 82 (1985) 6774–6778.
[14] D.K. Orren, C.P. Selby, J.E. Hearst, A. Sancar, Post-incision steps of nucleotide excision repair in *Escherichia coli*. Dis-

assembly of the UvrBC-DNA complex by helicase II and DNA polymerase I. J. Biol. Chem. 267 (1992) 780–788.
[15] C.P. Selby, A. Sancar, Molecular mechanism of transcription-repair coupling, Science 260 (1993) 53–58.
[16] I. Gordienko, W.D. Rupp, UvrAB activity at a damaged DNA site: is unpaired DNA present?, EMBO J. 16 (1997) 880–888.
[17] R.S. Lloyd, B. Van Houten, DNA damage recognition, in: J.-M. Vos (Ed.), DNA Repair Mechanisms: Impact on Human Diseases and Cancer, R.G. Landes, Biomedical Publishers, Austin, TX, 1995, pp. 25–66.
[18] N. Goosen, G.F. Moolenaar, R. Visse, P.V.D. Putte, Functional domains of the *E. coli* UvrABC proteins in nucleotide excision repair, in: F. Eckstein, D.M.J. Lilley (Eds.), Nucleic Acids and Molecular Biology vol. 12 Springer-Verlag, Berlin, 1998, pp. 103–123.
[19] E.Y. Oh, L. Grossman, Helicase properties of the *Escherichia coli* UvrAB protein complex, Proc. Natl. Acad. Sci. U.S.A. 84 (1987) 3638–3642.
[20] T.W. Seeley, L. Grossman, Mutations in the *Escherichia coli* UvrB ATPase motif compromise excision repair capacity, Proc. Natl. Acad. Sci. U.S.A. 86 (1989) 6577–6581.
[21] M. Machius, L. Henry, M. Palnitkar, J. Deisenhofer, Crystal structure of the DNA nucleotide excision repair enzyme UvrB from *Thermus thermophilus*, Proc. Natl. Acad. Sci. U.S.A. 96 (1999) 11717–11722.
[22] N. Nakagawa, M. Sugahara, R. Masui, R. Kato, K. Fukuyama, S. Kuramitsu, Crystal structure of *Thermus thermophilus* HB8 UvrB protein, a key enzyme of nucleotide excision repair, J. Biochem. 126 (1999) 986–990.
[23] K. Theis, P.J. Chen, M. Skorvaga, B.V. Houten, C. Kisker, Crystal structure of UvrB, a DNA helicase adapted for nucleotide excision repair, EMBO J. 18 (1999) 6899–6907.
[24] M. Sohi, A. Alexandrovich, G. Moolenaar, R. Visse, N. Goosen, X. Vernede, J. Fontecilla-Camps, J. Champness, M.R. Sanderson, Crystal structure of *Escherichia coli* UvrB C-terminal domain, and a model for UvrB–UvrC interaction, FEBS Lett. 465 (2000) 161–164.
[25] E.C. Friedberg, G.C. Walker, W. Siede, DNA Repair and Mutagenesis. ASM Press, Washington, DC, 1995.
[26] L. Grossman, C.I. Lin, Y. Ahn, Nucleotide excision repair in *Escherichia coli*, in: J.A. Nickoloff, M.F. Hoekstra (Eds.), DNA Damage and Repair vol. 1 Humana Press, Totowas, NJ, 1998, pp. 11–27.
[27] A. Sancar, DNA excision repair, Annu. Rev. Biochem. 65 (1996) 43–81.
[28] A. Alexandrovich, M.R. Sanderson, G. Moolenaar, N. Goosen, A.N. Lane, NMR assignments and secondary structure of the UvrC binding domain of UvrB, FEBS Lett. 451 (1999) 181–185.
[29] A. Shibata, N. Nakagawa, M. Sugahara, R. Masui, R. Kato, S. Kuramitsu, K. Fukuyama, Crystallization and preliminary X-ray diffraction studies of a DNA excision repair enzyme, UvrB, from *Thermus thermophilus* HB8, Acta Cryst. D55 (1999) 704–705.
[30] A.E. Gorbalenya, E.V. Koonin, A.P. Donchenko, V.M. Blinov, Two related superfamilies of putative helicases involved in replication, recombination, repair and expression of DNA and RNA genomes, Nucleic Acids. Res. 17 (1989) 4713–4730.
[31] L. Holm, C. Sander, Dali: a network tool for protein structure comparison, Trends Biochem. Sci. 20 (1995) 478–480.
[32] J.L. Kim, K.A. Morgenstern, J.P. Griffith, M.D. Dwyer, J.A. Thomson, M.A. Murcko, C. Lin, P.R. Caron, Hepatitis C virus NS3 RNA helicase domain with a bound oligonucleotide: the crystal structure provides insights into the mode of unwinding, Structure 6 (1998) 89–100.
[33] S. Korolev, J. Hsieh, G.H. Gauss, T.M. Lohmann, G. Waksman, Major domain swiveling revealed by the crystal structures of complexes of *E. coli* Rep Helicase bound to single-stranded DNA and ADP, Cell 90 (1997) 635–647.
[34] S.S. Velankar, P. Soultanas, M.S. Dillingham, H.S. Subramanya, D.B. Wigley, Crystal structures of complexes of PcrA DNA helicase with a DNA substrate indicate an inchworm mechanism, Cell 97 (1999) 75–84.
[35] S. Korolev, N.H. Yao, T.M. Lohman, P.C. Weber, G. Waksman, Comparisons between the structures of HCV and Rep helicases reveal structural similarities between SF1 and SF2 super-families of helicases, Protein Sci. 7 (1998) 605–610.
[36] T.W. Seeley, L. Grossman, The role of *Escherichia coli* UvrB in nucleotide excision repair, J. Biol. Chem. 265 (1990) 7158–7165.
[37] P.R. Caron, L. Grossman, Involvement of a cryptic ATPase activity of UvrB and its proteolysis product, UvrB*, in DNA repair, Nucleic Acids Res. 16 (1988) 9651–9662.
[38] I. Gordienko, W.D. Rupp, The limited strand-separating activity of the UvrAB protein complex and its role in the recognition of DNA damage, EMBO J. 16 (1997) 889–895.
[39] M. Hall, S. Matson, Helicase motifs: the engine that powers DNA unwinding, Mol. Microbiol. 34 (1999) 867–877.
[40] J.E. Walker, M. Saraste, M.J. Runswick, N.J. Gay, Distantly related sequences in the a- and b-subunits of ATP synthase, myosin, kinases, and other ATP-requiring enzymes and a common nucleotide binding fold, EMBO J. 1 (1982) 945–951.
[41] R. Kato, N. Yamamoto, K. Kito, S. Kuramitsu, ATPase activity of UvrB protein from *Thermus thermophilus* HB8 and its interaction with DNA, J. Biol. Chem. 16 (1996) 9612–9618.
[42] E.L. Hildebrand, L. Grossman, Introduction of a tryptophan reporter group into the ATP binding motif of the *Escherichia coli* UvrB protein for the study of nucleotide binding and conformational studies, J. Biol. Chem. 273 (1998) 7818–7827.
[43] H.S. Koo, L. Claassen, L. Grossman, L.F. Liu, ATP-dependent partitioning of the DNA template into supercoiled domains by *Escherichia coli* UvrAB, Proc. Natl. Acad. Sci. U.S.A. 88 (1991) 1212–1216.
[44] O.I. Kovalsky, L. Grossman, B. Ahn, The topodynamics of incision of UV-irradiated covalently closed DNA by the *Escherichia coli* Uvr(A)BC endonuclease, J. Biol. Chem. 52 (1996) 33236–33241.

[45] G.F. Moolenaar, R. Visse, M. Ortiz-Buysse, N. Goosen, P. van de Putte, Helicase motifs V and VI of the *Escherichia coli* UvrB protein of the UvrABC endonuclease are essential for the formation of the preincision complex, J. Mol. Biol. 240 (1994) 294–307.

[46] G.F. Moolenaar, M.F.P. Herron, V. Monaco, G.A. van der Marel, J.H. van Boom, R. Visse, N. Goosen, The role of ATP binding and hydrolysis by UvrB during nucleotide excision repair, J. Biol. Chem. 275 (2000) 8044–8050.

[47] Y. Zou, R. Walker, H. Bassett, N.E. Geacintov, B.V. Houten, Formation of DNA repair intermediates and incision by the ATP-dependent UvrB–UvrC endonuclease, J. Biol. Chem. 272 (1997) 4820–4827.

[48] G.F. Moolenaar, V. Monaco, G.A. van der Marel, J.H. van Boom, R. Visse, N. Goosen, The effect of the DNA flanking the lesion on formation of the UvrB–DNA preincision complex, J. Biol. Chem. 275 (2000) 8038–8043.

[49] P. Soultanas, M.S. Dillingham, S.S. Velankar, D.B. Wigley, DNA binding mediates conformational changes and metal ion coordination in the active site of PcrA helicase, J. Mol. Biol. 290 (1999) 137–148.

[50] D.S. Hsu, S.-T. Kim, Q. Sun, A. Sancar, Structure and function of the UvrB protein, J. Biol. Chem. 270 (1995) 8319–8327.

[51] G.F. Moolenaar, K.L.M.C. Franken, D.M. Dijkstra, J.E. Thomas-Oates, R. Visse, P. van de Putte, N. Goosen, The C-terminal region of the UvrB protein of *Escherichia coli* contains an important determinant for UvrC binding to the preincision complex but not the catalytic site for 3'-incision, J. Biol. Chem. 270 (1995) 30508–30515.

[52] G.F. Moolenaar, K.L.M.C. Franken, P. van de Putte, N. Goosen, Function of the homologous regions of the *Escherichia coli* DNA excision repair proteins UvrB and UvrC in stabilization of the UvrBC-DNA complex and in 3'-incision, Mutat. Res. 385 (1997) 195–203.

[53] G.F. Moolenaar, M. Bazuine, I.C. van Knippenberg, R. Visse, N. Goosen, Characterization of the *Escherichia coli* damage-independent UvrBC endonuclease activity, J. Biol. Chem. 273 (1998) 34896–34903.

[54] N. Nakagawa, R. Masui, R. Kato, S. Kuramitsu, Domain structure of *Thermus thermophilus* UvrB protein — similarity in domain structure to a helicase, J. Biol. Chem. 272 (1997) 22703–22713.

[55] S.J. Mazur, L. Grossman, Dimerization of *Escherichia coli* UvrA and its binding to undamaged and ultraviolet light damaged DNA, Biochemistry 30 (1991) 4432–4443.

[56] B. Ahn, L. Grossman, The binding of UvrAB proteins to bubble and loop regions in duplex DNA, J. Biol. Chem. 271 (1996) 21462–21470.

[57] Y. Zou, B. Van Houten, Strand opening by the UvrA$_2$B complex allows dynamic recognition of DNA damage, EMBO J. 18 (1999) 4889–4901.

[58] I. Gordienko, W.D. Rupp, A specific 3' exonuclease activity of UvrABC, EMBO J. 17 (1998) 626–633.

[59] G.F. Moolenaar, R.S. Uiterkamp, D.A. Zwijnenburg, N. Goosen, The C-terminal region of the *Escherichia coli* UvrC protein, which is homologous to the C-terminal region of the human ERCC1 protein, is involved in DNA binding and 5' incision, Nucleic Acids Res. 26 (1998) 462–468.

[60] J.J. Lin, A.M. Phillips, J.E. Hearst, A. Sancar, Active site of (A)BC excinuclease: II. Binding, bending and catalysis mutants of UvrB reveal a direct role in 3' and an indirect role in 5' incision, J. Biol. Chem. 267 (1992) 17693–17700.

[61] D.G. Vassylyev, T. Kashiwagi, Y. Mikami, M. Ariyoshi, S.O. Iwai, E.K. Morikawa, Atomic model of a pyrimidine dimer excision repair enzyme complexed with a DNA substrate: structural basis for damaged DNA recognition, Cell 83 (1995) 773–782.

[62] B. Van Houten, H. Gamper, S.R. Holbrook, J.E. Hearst, A. Sancar, Action mechanism of ABC excision nuclease on an DNA substrate containing a psoralen crosslink at a defined position, Proc. Natl. Acad. Sci. U.S.A. 83 (1986) 8077–8081.

[63] E.Y. Oh, L. Grossman, Characterization of the helicase activity of the *Escherichia coli* UvrAB protein complex, J. Biol. Chem. 264 (1989) 1336–1343.

[64] S. Thiagalingam, L. Grossman, The multiple roles for ATP in the *Escherichia coli* UvrABC endonuclease-catalyzed incision reaction, J. Biol. Chem. 268 (1993) 18382–18389.

[65] P.J. Kraulis, MOLSCRIPT — a program to produce both detailed and schematic plots of protein structures, J. Appl. Cryst. 24 (1991) 946–950.

[66] E.A. Merritt, M.E.P. Murphy, Raster3D Version 2.0 — a program for photorealistic molecular graphics, Acta Cryst. D50 (1994) 869–873, (Nov).

[67] G.J. Barton, ALSCRIPT: a tool to format multiple sequence alignments, Protein Eng. 6 (1993) 37–40.

[68] J.D. Thompson, D.G. Higgins, T.J. Gibson, CLUSTAL W: improving the sensitivity of progressive multiple sequence alignment through sequence weighting, position-specific gap penalties and weight matrix choice, Nucleic Acids Res. 22 (1994) 4673–4680.

[69] A. Bairoch, R. Apweiler, The SWISS-PROT protein sequence database and its supplement TrEMBL in 2000, Nucleic Acids Res. 28 (2000) 45–48.

[70] A. Nicholls, K.A. Sharp, B. Honig, Protein folding and association: insights from the interfacial and thermodynamic properties of hydrocarbons, Proteins 11 (1991) 281–296.

[71] B. Van Houten, Mechanism of action of the *Escherichia coli* UvrABC nuclease: clues to the damage recognition problem, Bioessays 15 (1993) 51–59.

[72] G. Duval-Valentin, M. Takasugi, C. Hélène, E. Sage, Triple helix directed psoralen crosslinks are recognized by Uvr(A)BC Excinuclease, J. Mol. Biol. 1998 (1998) 815–825.